Mechanical Damage to Estabragh Fibers in the Production of Thermobonded Layers

Ali Akbar Gharehaghaji, Sara Hayat Davoodi

Department of Textile Engineering, Isfahan University of Technology, Isfahan 84156-83111, Iran

Received 26 June 2006; accepted 1 October 2007
DOI 10.1002/app.28230
Published online 21 May 2008 in Wiley InterScience (www.interscience.wiley.com).

ABSTRACT: Estabragh (*Asclepias procerais*) fibers are natural, hollow fibers, and the mechanical behavior of these fibers plays a major role in mechanical processing. This work explores the mechanical behavior of estabragh fibers in three different areas—tensile failure, carding behavior, and the construction of nonwoven layers—and reports the main barriers in the spinning process of these fibers. In the first step, a typical stress–strain curve of estabragh fibers is plotted. Fractography of the broken ends by scanning electron microscopy shows the granular nature of the fracture. The likely mechanism of tensile failure is discussed and compared with the fracture of cotton fibers under tensile loading. In the second stage, the carding behavior and likely mechanism of fiber damage during the carding process of estabragh fibers are studied. Both qualitative and quantitative studies show that estabragh fibers experience serious damage during the carding process. The effect of the hollowness of the fibers on their mechanical properties is discussed as well. In the final approach, thermobonded layers of two different blends of estabragh fibers and bicomponent poly(ethylene terephthalate) fibers are produced. Some properties of the produced layers, including moisture absorption, ultraviolet absorption, and bending length, are reported. © 2008 Wiley Periodicals, Inc. J Appl Polym Sci 109: 3062–3069, 2008

Key words: electron microscopy; fracture; mechanical properties; tension

INTRODUCTION

Estabragh fibers are fibers of seed vegetables that are planted in desert areas in the southern region of Iran. The fibers grow in groups inside the seed, and each staple contains uniform, longitudinally oriented fibers. The fibers are straight, and there is no crimping along the fiber length; this may lead to several barriers in processing and can affect the spinning of fibers. The silky luster and hollowness of these fibers resemble milkweed (*Asclepias syriaca*) fibers.[1] According to historical evidence, beautiful cloth called Dibayeh Shooshtari was woven from the yarns of these fibers.[2] In a previous work,[3] some mechanical and physical properties of estabragh fibers have been studied. Also, the fracture of these fibers under tensile loading has been reported already.[4] The fractured surface of these fibers is presented in the atlas of fiber fracture as well.[5] In a previous work, the physical and mechanical properties and dyeing behavior of milkweed fibers have been studied and compared with those of cotton, wool, and rabbit hair fibers.[6]

Estabragh fibers experience the same difficulties that milkweed fibers undergo during the spinning process[7] because the fibers are straight and crimpled, and this makes control of the fibers more difficult during the various stages of spinning and especially during the carding process. The fibers are hollow in nature, and the ratio of the hollow area to the fibrous area is considerable. The hollowness of the fibers governs the mechanical behavior in tension and bending. In tension, the tensile strength weakens because of the reduced resistant area. In the bending of estabragh fibers, the maximum bending stress is expected to be higher than that of fibers without a cavity but with the same fibrous area.[8]

For the spinning of estabragh fibers, exploring their carding behavior and mechanical damage and the mechanism of mechanical fracture is essential. The study of the fractured area of estabragh fibers broken under tensile loading has not received enough consideration in the literature. The studies are restricted to showing examples of failure.[2,5] The study of fractured areas in more detail may provide a better understanding of the behavior of estabragh fibers in tension. This work was designed to find the likely mechanism of estabragh fiber failure and the effect of hollowness on the mechanical behavior. In this investigation, a scanning electron microscopy (SEM) study was used to assess and reveal the mechanical damage in the carding process and the behavior of estabragh fibers in tensile loading. Ther-

Correspondence to: A. A. Gharehaghaji (aghaji@cc.iut.ac.ir).
Contract grant sponsor: Research Affairs of the Isfahan University of Technology.

© 2008 Wiley Periodicals, Inc.

mobonded layers of blends of estabragh fibers and bicomponent poly(ethylene terephthalate) (PET) fibers were produced in a sample roller card. Various properties of sample layers, such as moisture absorption, ultraviolet (UV) absorption, and bending length, were studied and are reported.

EXPERIMENTAL

Estabragh fibers were used in this work, and they were supplied by the Natural Resources Research Organization (Ahwaz, Iran). Also, bicomponent PET fibers were supplied by DuPont Co. (Wilmington, DE) (staple length = 38 mm, linear density = 1.5 den). The specifications of the estabragh fibers are listed in Table I. The mean diameter of the estabragh fibers was 18.3 μm, which was assessed with a Projectina microscope (Heerbrugg, Switzerland) through the examination of 560 specimens.

Tensile behavior of estabragh fibers under tensile loading

To study the mechanism of mechanical fracture under tensile loading, the experiment was conducted with a Zwick tensile tester (model 1446, Zwick/Materiol Prufung, Ulm, Germany) with a paperboard sample holder clamped in the lower and top jaws. For assessing the tensile strength, 80 individual test fibers were randomly chosen and mounted across the 10-mm gap of the sample holder (gauge length = 10 mm, crosshead speed = 1.5 mm/min), which was wrapped with double-sided tape. Special care was taken for any extensions of the fibers before the test. The most important requirement of this experiment was to avoid tensioning the fiber before it was stretched in the Zwick tensile tester. Because the test fiber was straight and crimpled, the fiber was laid easily on the paperboard. The rest of the paperboard was cut away carefully, and the fiber was ready for testing. Figure 1 shows typical strain–stress curves of estabragh fibers. Consequently, the broken ends were prepared for SEM examinations.

The fractured ends of some specimens of the 80 test fibers were randomly chosen and prepared for SEM studies. The test fibers were first coated with gold in a sputter coater to prevent surface charging in the electron beam. A Philips XL30 scanning electron microscope (Eindhoven, The Netherlands) was used in this study to reveal the details of the surface, cross-sectional area, and fracture surface of the fiber through the SEM studies. A low accelerating voltage (5 kV) was adopted to minimize beam damage to the fiber. Also, low magnification was used for better resolution of the pictures and reduction of sample damage. To investigate the mode of failure, the samples were studied carefully in different directions. The results of these observations are presented in Figure 2(a–d).

TABLE I
Specifications of Estabragh Fibers

	Mean length (mm)	Fineness (dtex)	Strength (cN/dtex)	Elongation (%)
Estabragh fibers	33.5	1.72	3.056	2.2
Plasma-treated estabragh fibers	33.5	1.72	1.9	2

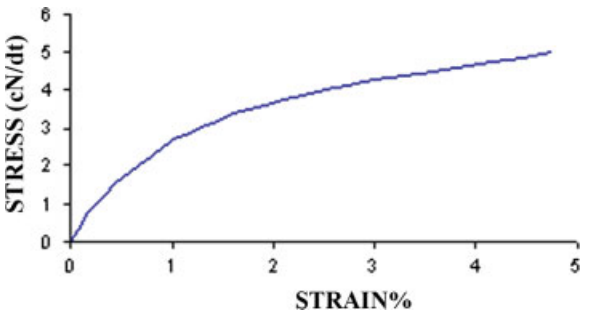

Figure 1 Typical stress–strain behavior of estabragh fibers under tensile loading. [Color figure can be viewed in the online issue, which is available at www.interscience.wiley.com.]

Study of the carding behavior

Two different blends of estabragh and PET were produced, that is, 90/10 and 80/20 blends (weight percentage ratios). In both cases, the fibers first were blended manually, and then they were put under conditioning for 48 h after spinning oil with a 1.5% concentration was sprayed. Before the blended fibers were fed into the woolen sample card, the samples of 100% estabragh fibers consisted of two groups of fibers: fibers with 1.5% spinning oil and fibers without it. The examination showed that carding of the estabragh fibers without spinning oil was almost impossible, and a high extent of fiber drop occurred.

Both flat and roller cards were used in this study; the latter was more successful in processing. This could be attributed to the great power of the roller card in fiber blending. The roller card was a sample woolen card. After the carding process, the percentages of dropping fibers were measured, and they are listed in Table II.

For a better evaluation of the effect of the carding process on damage to estabragh fibers, the mean length of the fibers was measured before and after carding. Also, the mean tenacity and elongation of the fibers were assessed. Table II shows the percentages of the reduction in the fiber tenacity and fiber mean length. A paired t test was used for statistical analysis of the results. The statistical assessment showed that there was a significant different between the fiber tenacity before and after carding at

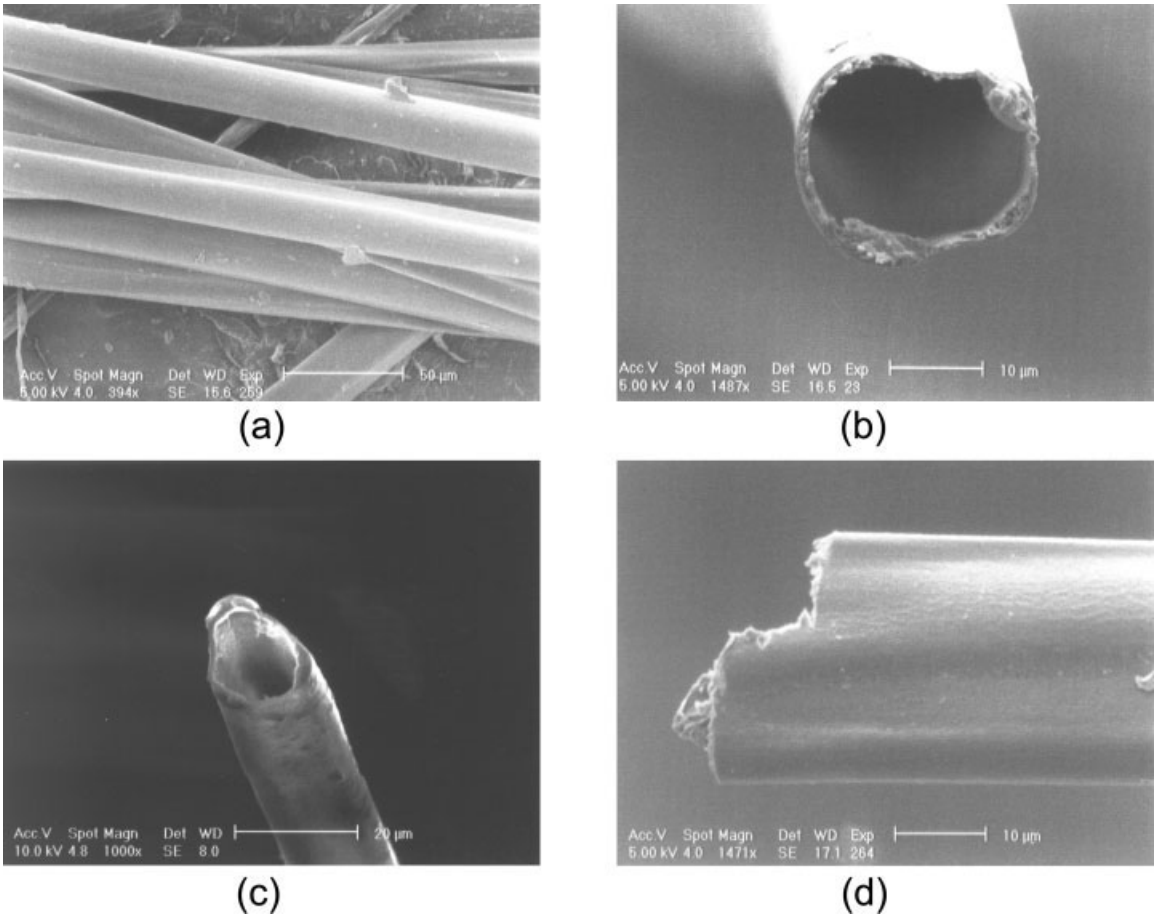

Figure 2 (a) Surface morphology of estabragh fibers, (b) cross section of an estabragh fiber, (c) fractured surface morphology of an estabragh fiber after tensile loading and breaking, and (d) an estabragh fiber after tensile loading.

the 95% confidence level. Figures 3(a–e) and 4(a–e) demonstrate some features of fiber webs, fiber damage, and fiber fracture captured through SEM studies.

Properties of nonwoven layers

After batt formation in front of the card, it was cut carefully into a square shape with dimensions of 20 cm × 20 cm, and its mass was measured. These layers consequently were put between two Teflon-coated plates and then were put into an oven. Although the compressing dead weights, duration of thermal treatment, and treatment temperature could be considered as variables, in this work, the layers were put for 5 min in the oven, the temperature of which was initially set to 140°C. These values were according to a study already reported.[9] Some properties of the produced layers, including moisture absorption, UV absorption, and bending length, have been studied and reported.

UV absorption

To study the UV absorption of the layers, samples with dimensions of 5 cm × 15 cm were prepared. Tests on the thermobonded layers were carried out with xenon. A sun test lamp was used to simulate sun photographs. After 48 h of exposure of the layers to this light, the UV absorption of the layers was measured with a spectrophotometer.

TABLE II
Estabragh Fiber Behavior During Carding

	Dropping of estabragh fibers under various conditions (%)	Reduction in the tenacity of estabragh fibers (%)	Reduction in the mean length of estabragh fibers (%)
100% estabragh fibers with 1.5% spinning oil	55.5	5.3	49.1
90/10 estabragh/PET	50	16	47.7
80/20 estabragh/PET	15.5	10.2	40.5

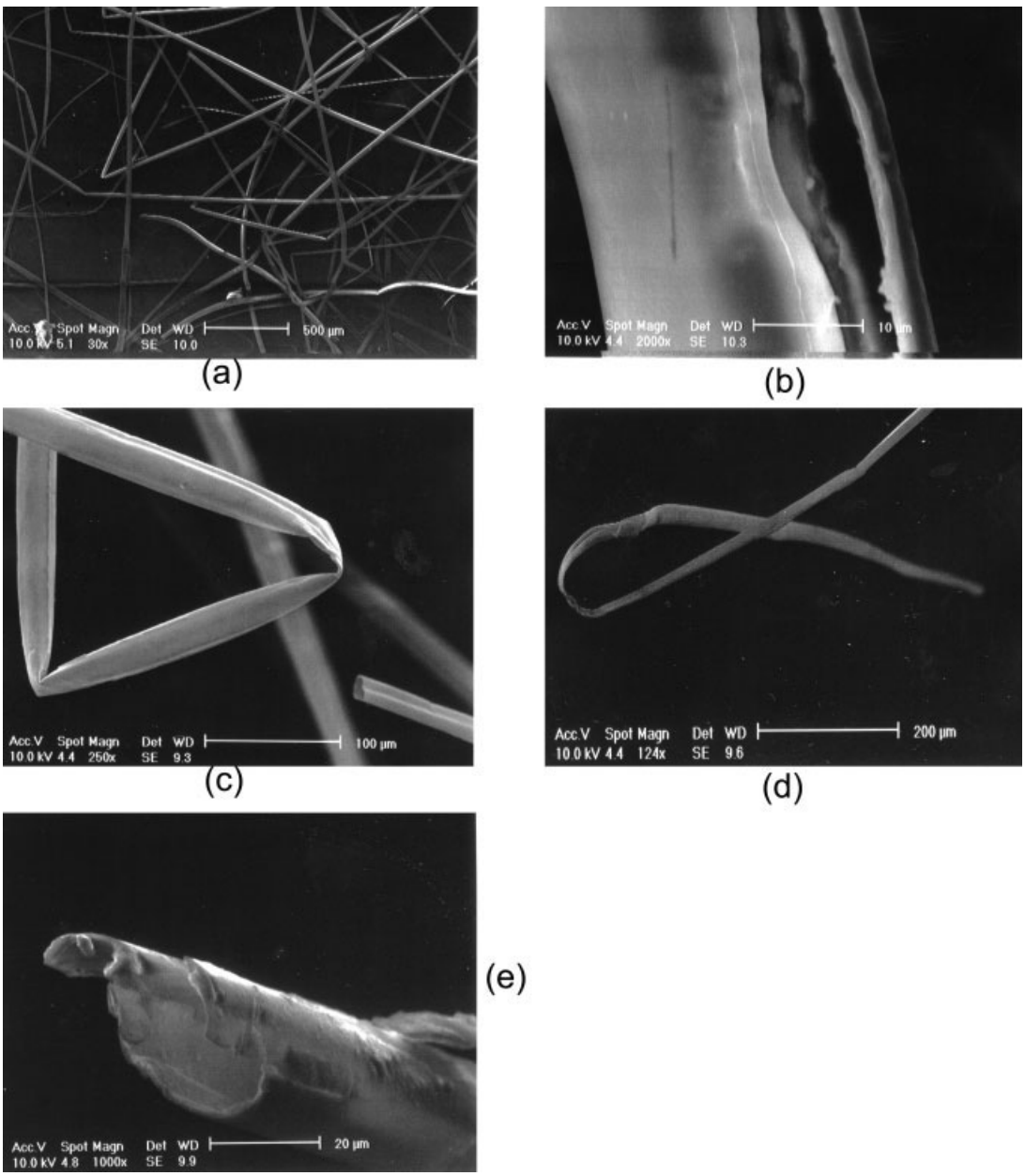

Figure 3 (a) General view of a web of estabragh fibers, (b) outer surface of a fractured estabragh fiber, (c) bending of a estabragh fiber in two positions, (d) trailing hook of a estabragh fiber, and (e) small transverse cracks and crack growth,

Bending rigidity

The bending length of the layers was measured with a drape tester. The angle of the instrument was 41.5°, and the bending length [c (cm)] was measured with the following equations:

$$c = lf(\theta)$$

$$f(\theta) = \left(\frac{\cos\frac{\theta}{2}}{8tg\theta}\right)^{\frac{1}{3}}$$

where $f(\theta)$ is the function of theta, and l is the specimen length.

The bending length was 3.72 cm (the mean of 10 tests), and the layer thickness was 0.37 mm (the mean of 10 tests). The bending rigidity has a determining effect on the handle of fibrous structures such as thermobonded layers. In this study, the bending rigidity of the layers was measured with the following equation and is shown in Figure 5:

$$G = WC^3 \times 10^3$$

where G is the bending rigidity, W is the specimen weight, and C is the bending length.

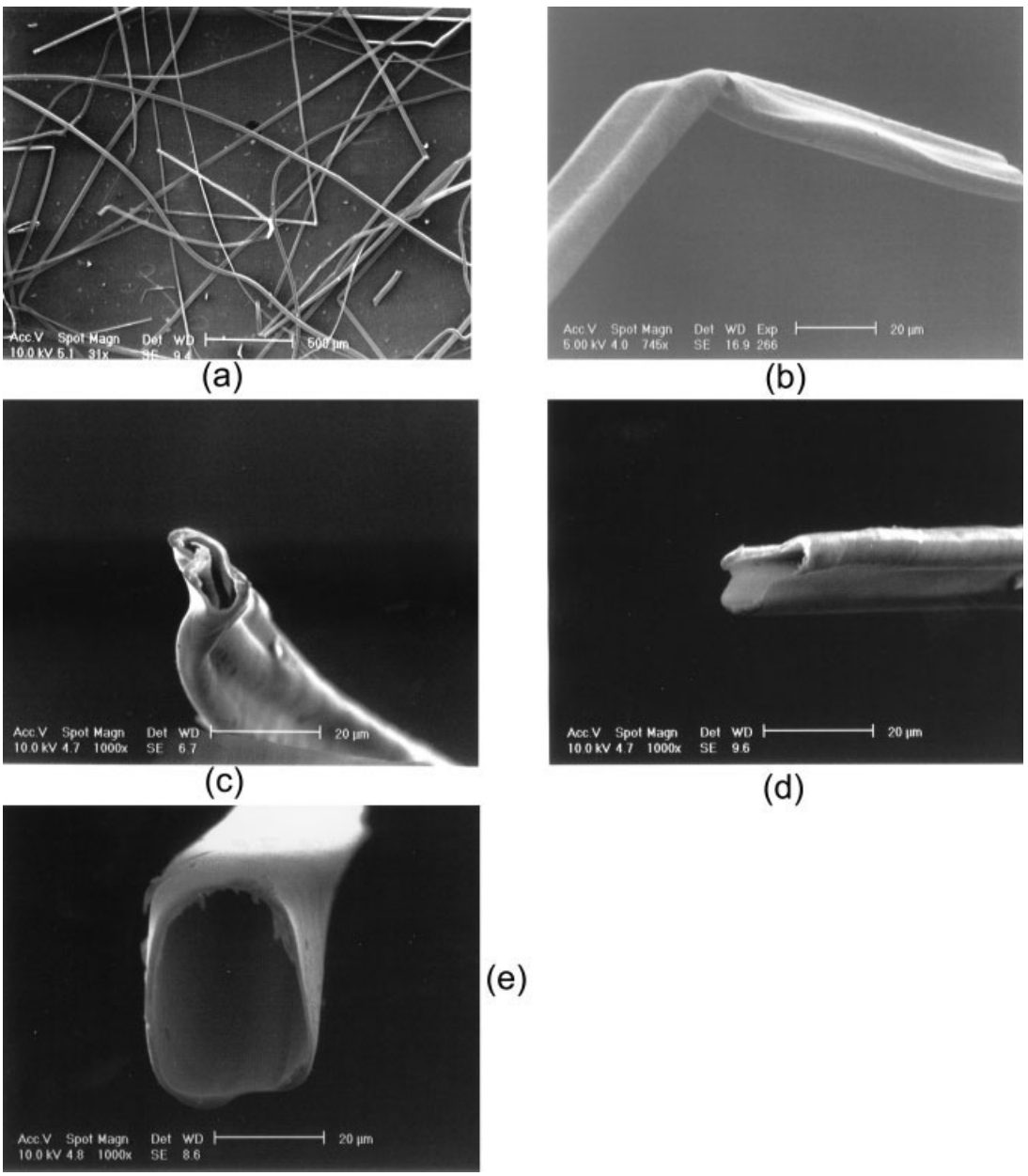

Figure 4 (a) General view of a web, (b) bending of an estabragh fiber, (c) buckling view of an estabragh fiber, (d) damaged estabragh fiber, and (e) cross section of a fractured estabragh fiber.

Moisture absorption

The moisture absorption of estabragh/PET layers was measured and compared with that of a 100% cotton layer with the same mass and dimensions.

Cold plasma treatment

This treatment was carried out to initiate surface roughness, which was necessary during spinning because of the lack of crimping. It was designed to increase the cohesion between fibers both to enhance the friction between the fibers and to reduce fiber drop during the carding process. The plasma treatment was carried out on physical vapour deposition (PVD) for 15 min with nitrogen gas by the adjustment of the power and vacuum pressure. Table I shows the elongation and tenacity after the plasma treatment. Figure 6(a,b) presents the surface changes on the estabragh fibers after the plasma treatment.

RESULTS AND DISCUSSION

Tensile behavior of estabragh fibers under tensile loading

During the examination of the cross-sectional area of the fibers under SEM, it was found that the fibrous

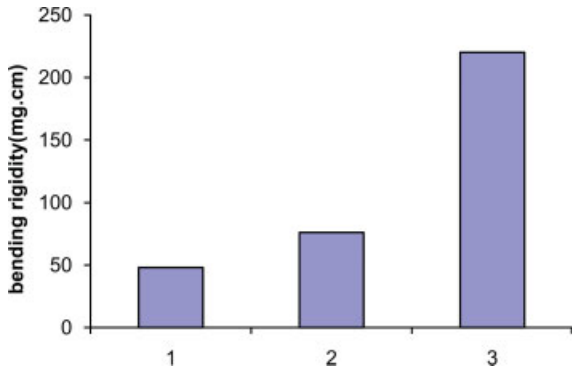

Figure 5 Bending rigidity of various layers: (1) estabragh/PET (80/20), (2) hetrofil/hemofil (65/35), and (3) polyester/polypropylene layers (65/35). [Color figure can be viewed in the online issue, which is available at www.interscience.wiley.com.]

part of the fiber is almost 44% of the whole fiber, and the rest is the hollow part (by the measurement of the area). Considering the density of the estabragh fibers measured during this work (1.46 g/cm) and their hollowness, we determined the linear density of the fibers to be 1.72 dtex. These studies show that the fibers have good uniformity in their length and fineness. The SEM study of the surface morphology of the fibers before stretching shows that they are initially undamaged before the tensioning process.

The stress–strain behavior of the estabragh fibers shows some discrepancy in comparison with the curve of cotton fibers. Although the tenacity is about that of St. Vincent cotton fibers, the breaking extension is lower than the breaking extension of Bengal cotton.[10] This can be attributed to the differences in the orientation of the molecular arrangement, hollowness, shape of the resistant area, and crystallinity.

SEM studies of the fiber strand [Fig. 2(a)] and cross section of estabragh fibers before stretching [Fig. 2(b)], show that the fibers are undamaged before mechanical processing, and the cross-sectional area is elliptic. This elliptical area resembles wool fibers and slightly differs from a figure shown in a previous work.[5] It seems that the fiber in the so-called study has been flattened somehow. The surface morphology shows a smooth surface [Fig. 2(a)] with some concaveness [Fig. 2(b)]. This concavity seems to be affected by the variable thickness of the fibrous part in the inner surface, as can be seen in Figure 2(b).

Figure 2(c) shows a test fiber after tensile loading and breaking (this specimen was a strong fiber with a tenacity of 5.8 cN/dtex). After the stretching of the fiber, the elliptical resistant area deformed to a rectangular shape with curved corners. This could be attributed to the variable thickness of the fibrous material of the resistant area, which led to a variable distribution of the tensile stresses. Because the stress concentration occurred in the thin areas, a thin wall deformed from curved surfaces to flat surfaces, and the thick area remained the curved corner of the rectangle. This phenomenon can be clearly seen in Figure 2(c), which reflects the effects of the variable wall thickness.

Figure 2(d) shows another fractured surface morphology, and it could be indicative of the starting point of the fracture. It seems that the failure starts outside the fiber and develops inside it. As can be seen in Figures 2(c,d), the outer surface of the fracture has a relatively smooth surface, whereas the inner wall of the fracture area shows some protrusion of partial fracture. These features strengthen the possibility of the propagation of the partial fracture (i.e., crack) from outside the hollow fibers toward an inner wall.

SEM studies on the fractured surfaces show that the plane of fracture is almost perpendicular to the fiber axis. The fracture behavior of the fibers is indic-

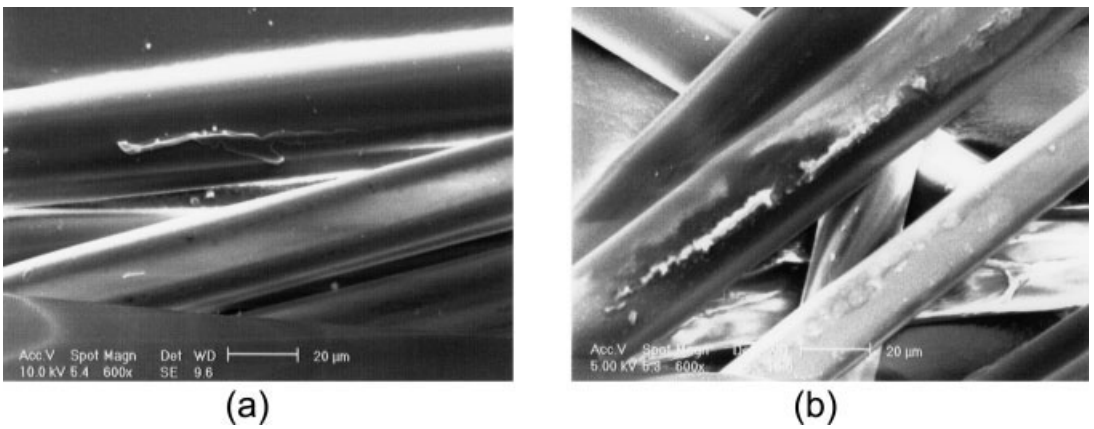

Figure 6 (a) Changes in the surface of estabragh fibers after cold plasma treatment and (b) severe surface corrosion of estabragh fibers after cold plasma treatment.

ative of granular fracture. In this fracture mode, a short length of separation links the transversely fractured zones together. This is one of the fracture features of cotton fibers in tensile loading as well.[5] The typical form of the tensile fracture of cotton fibers shows a longitudinal crack that develops around the fiber and then tears back along the fiber.[5] Different fracture patterns of cotton fiber are generally in granular and fibrillar modes. SEM results on the breaking form of estabragh fibers (granular fracture) are consistent with the results reported by Hearle et al.[5] This reflects the different internal structure of the estabragh and cotton fibers. It seems that unlike cotton fibers, unicellular estabragh seed fibers have a much more highly oriented molecular arrangement. This can limit the tensile fracture mode of estabragh fibers to granular fracture. In polyester hollow fibers, tensioning leads to a modified form of ductile failure.[5]

Carding behavior of estabragh fibers

The carding behavior of estabragh fibers was affected by the bicomponent PET fibers in the blend, and the damaging effect of carding and estabragh fiber dropping decreased considerably when the share of the PET fibers increased to 20% (Table II). This phenomenon indicates that PET fibers could have better control on the crimples straight estabragh fibres during carding. Also, these fibers may have supported the estabragh fibers against mechanical damage, which could cause shortening of the fibers. Consequently, thermobonded layers were produced from this blend.

SEM studies could reveal some features of damage during the mechanical processing of estabragh fibers. Figure 3(a) show a general view of a random region of the web. This general view demonstrates fiber bending with a sharp angle clearly. However, there is a great lack of neps and end hooks (which constitute less than 20% of the fibers). This is in agreement with a previous study.[6]

Some of the fibers were broken because of the impact with the pin (clothing surface of the carding frame) and moving rollers in the carding action. Figure 3(b) shows the severe damaging effect of the pin, which has torn the fiber surface in the longitudinal direction. In this figure, a longitudinal crack can be seen. This crack started at one point and then grew along the axis of the fiber. Crack growth in this axis could be attributed to internal surfaces of these fibers. The other feature is the effect of contact stresses that build up on the fiber surface in the form of compressive deformation. Trajectories of pressure can be seen in this figure. Flattened walls and exposure of the inner fibrous materials are common features in most of the failure evidence.

Figure 3(c) shows the bending behavior of the fibers. Flattening at the bend is typical in these fibers. This figure shows fiber bending in two positions. One could consider that in this position the fibers become completely flattened. If the fibers were not hollow and the fibrous material did not flatten, they would become hooks because of the pressure and successive bending stresses. Flattening at the bend is typical in these fibers.

We could observe only one end hook in this web sample [Fig. 3(d)], which may have been formed during the transfer of the fiber from one clothing surface to another. As Figure 3(e) demonstrates, breakage starts from one point, and then a crack grows in such a way that breakage occurs along the fiber axis. A small transverse crack exists on the surface of the fiber. This type of crack may be the initial cite for crack growth and catastrophic failure when the fiber undergoes tensioning.

Figure 4(a) shows another web sample of the estabragh/PET blend. Figure 4(b) shows the bending position of the fiber. In this figure, the fiber is completely curled, and a sharp angle is created by the collapse of the fiber wall.

Figure 4(c) illustrates the buckling of the fiber after the removal of the tensile load and its fracture. The grooves on the longitudinal surface show the deformation after the buckling of the fiber. This state (buckling after the removal of tensile stresses) may be due to the absorption of spinning oil by the fiber, which in return could increase fiber flexibility. Grooves can be seen in Figure 4(d) as well.

In Figure 4(e), the fractured area (fiber cross section) and granular state are obvious. In this sample, the geometry of the fiber cross section has changed from an elliptical shape to a rectangular shape with sharp angles. In this figure, the fibrous wall seems to be thinner in some sections and thicker in other sections. This deformation and shape transformation from an ellipse to a rectangle can be attributed to the thickness differences in the fibrous section of this sample. This phenomenon (different wall thickness) could cause uneven distribution of tensile stresses on the bulk of the fiber. This could lead to stress concentration on the thin wall areas.

Cold plasma treatment

From a comparison of the plasma-treated and virgin estabragh fibers, it can be concluded that both the tenacity and breaking elongation are reduced. This indicates the damaging effect of plasma treatment on the estabragh fibers. The reduction in the tenacity is more pronounced, and paired t tests confirm that there is a significant difference between the mean fiber tenacity and breaking elongation at the 95% confidence level. Surface corrosion occurred on the

surface of the fibers, as can be seen in Figure 6(a,b). Figure 6(b) indicates severe corrosion of the surface due to the plasma treatment. The porosity of the surface was increased by the plasma treatment. The result suggests that surface modification by plasma treatment is not a suitable approach for increasing the cohesion between the estabragh fibers.

Properties of thermobonded layers

According to the findings of the bending tests (Fig. 5), the estabragh/PET layer has the lowest bending rigidity. The bending rigidity of the fibers, the shape of the cross-sectional area, the thickness of the layers, and the density of the layers play important roles in this respect. In these tests, the thickness of the estabragh/PET was more than that of hetrofil/hemofil and polypropylene/PET layers. The properties of these layers have been reported in a previous work.[9] It seems that during the formation of the thermobonded layers, estabragh fibers do not experience flattening under compression, whereas polypropylene/PET layers experience extreme changes in the cross-sectional area.

The moisture absorption of the layers was about 2% more than that of the layers of pure cotton with the same mass. This could have been affected by the hollowness of the fibers and their inner structure.

The results of the UV protection tests of the layers show that the estabragh/PET layer has a higher sun protection factor (SPF) than cotton fabrics. To assess the effect of the presence of PET fibers in the estabragh/PET layer on SPF, the SPF of a 100% estabragh layer was determined. The results show that the SPF of estabragh fibers is more than that of cotton fibers (SPF = 2) in both a pure estabragh layer (SPF = 3.07) and an estabragh/PET layer (SPF = 2.97).

CONCLUSIONS

A typical stress–strain curve of estabragh fibers has been derived from strength tests of the fibers and presented. The possible modes of fracture due to tensile stresses have been studied with SEM on single estabragh fibers that have been extended and fractured during the strength tests.

This study shows that the hollowness, variable thickness, and shape of the cross-sectional area of estabragh fibers mainly affect the fracture phenomenon. The elliptical cross section of the hollow fiber before tensioning deforms into a rectangular shape because of the stress concentration at the thin walls of the fiber when the fiber undergoes tensile stresses.

Fractography of the broken ends of estabragh fibers after stretching by SEM shows the granular break. Some fractured surfaces indicate that the fracture starts from the outer surface of the fiber and develops toward the inner surface in a plane perpendicular to the fiber axis.

In the carding process, the results show that the fiber shortening is decreased with the percentage of PET fibers increasing, but the mean tenacity shows a considerable drop in the fiber. This is indicative of serious fiber damage. The results of statistical tests and SEM evidence confirm this reduction in the tenacity. It seems that the number of estabragh fibers that are damaged by carding is low, but these fibers experience serious damage. Spinning oil may result in more flexibility of estabragh fibers, and in some instances, buckling may occur after the release of estabragh fibers from stretching.

An estabragh/PET layer shows lower bending rigidity that makes it more comfortable to use. The UV protection of estabragh fibers is higher than that of cotton, and this property could make estabragh fibers more useful in the sun protective clothing industry.

Although some surface roughness is produced by plasma treatment according to SEM data, this treatment also causes some drop in the tenacity and breaking elongation of estabragh fibers.

References

1. Louis, G.; Kottes Andrews, B. A. Text Res J 1987, 57, 339.
2. Sheikhzadeh Najar, S. M.Sc. Thesis, Amir Kabir University of Technology, 1989.
3. Haghighat Kish, M.; Shaikzadeh Najar, S. Int J Eng 1998, 1, 101.
4. Gharehaghaji, A. A.; Morshed, M. Proc Asian Text Conf 1997, 4, 64.
5. Hearle, J. W. S.; Lomas, B.; Looke, W. D.; Duerden, I. J. Fiber Failure and Wear of Materials; Wiley: Chichester, England, 1989.
6. Shakyawar, D. B.; Dagur, R. S.; Gupta, N. P. Indian J Fiber Text Res 1999, 24, 264.
7. Party, J.; Lombard, G.; Weltrowski, M. Text Res J 1993, 63, 443.
8. Popov, E. Introduction to Mechanics of Solids; Prentice Hall: Upper Saddle River, NJ, 1968; p 18.
9. Gharehaghaji, A. A.; Forughi, J. Int J Eng 2003, 16, 395.
10. Morton, W. E.; Hearle, J. W. S. Physical Properties of Textile Fibers, 3rd ed.; Textile Institute: Manchester, UK, 1993.